

# Fabrication of Conductive Macroporous Structures Through Nano-phase Separation Method

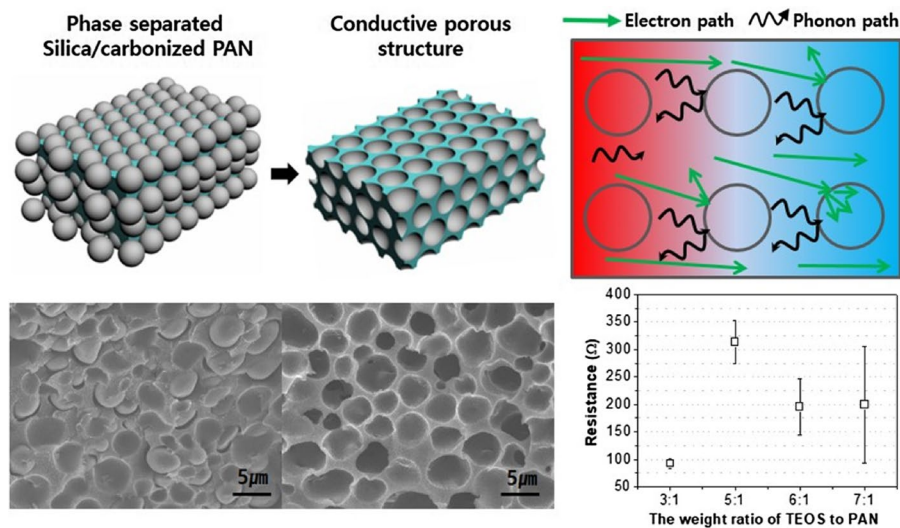
Soohyun Kim<sup>1</sup> · Hyunjung Lee<sup>1</sup>

Received: 24 April 2017 / Accepted: 26 June 2017 / Published online: 16 February 2018  
© The Korean Institute of Metals and Materials 2018

## Abstract

Thermoelectric power generation performance is characterized on the basis of the figure of merit, which tends to be high in thermoelectric materials with high electrical conductivity and low thermal conductivity. Porous structures cause phonon scattering, which decreases thermal conductivity. In this study, we fabricated porous structures for thermoelectric devices via nano-phase separation of silica particles from a polyacrylonitrile (PAN) matrix via a sol–gel process. The porosity was determined by control of silica particle size with various the mixing ratio of tetraethylorthosilicate as the precursor of silica particles to PAN. High electrical conductivity was maintained by subsequent carbonization of the PAN matrix in spite of a high porosity. As the results, the conductive porous structures having porosity from 13.9 to 83.3 (%) was successfully fabricated, keeping their electrical conductivities.

## Graphical Abstract



**Keywords** Conductive porous structure · Macroporous structure · Nanophase separation · Thermoelectric materials

## 1 Introduction

Porous structures are used in various energy devices, such as fuel cells, solar cells and so on because of the advantages provided by their structural characteristics [1–4]. Specially, the porous structure has advantage to decrease thermal conductivity as the thermoelectric materials [5].

✉ Hyunjung Lee  
hyunjung@kookmin.ac.kr

<sup>1</sup> School of Materials Science and Engineering, Kookmin University, Seoul 02707, Korea

Thermoelectric devices are energy conversion devices that operate by temperature gradient. When heat is applied to a thermoelectric device, the resulting transfer of charge carriers in the thermoelectric materials (*n*-type or *p*-type semiconductors) induced by the difference in temperature between the ends of the device generates electrical power. Thermoelectric power generation performance is characterized by the figure of merit ( $ZT$ ,  $ZT = (S^2\sigma/k)/T$ ). As expressed in the followed equation,  $ZT$  value is determined by the Seebeck coefficient ( $S$ ), the electrical conductivity ( $\sigma$ ), the thermal conductivity ( $\kappa$ ) and the absolute temperature ( $T$ ). Therefore, in order to obtain enhanced thermoelectric performance, low thermal conductivity as well as high power factor ( $PF = S^2\sigma$ ) is important as the thermoelectric materials.

Thermal conductivity is affected by an electric factor ( $\kappa_e$ ) and a lattice factor ( $\kappa_l$ ) ( $k = k_e + k_l$ ). The electric factor ( $\kappa_e$ ) represents thermal transfer by electrons and holes and is expressed by Wiedemann–Franz law ( $\kappa_e = L\sigma T = ne\mu LT$ ) [6]. As the Wiedemann–Franz law, the electric factor ( $\kappa_e$ ) of thermal conductivity is proportional to Lorenz number ( $L$ ,  $2.4 \times 10^{-8} \text{ J}^2 \text{ K}^{-1} \text{ C}^{-2}$ , free electrons), the electrical conductivity ( $\sigma$ ) and temperature ( $T$ ). Because electrical conductivity is determined by the charge of the electron ( $e$ ,  $1.6 \times 10^{-19} \text{ C}$ ), the carrier concentration ( $n$ ) and carrier mobility ( $\mu$ ), it is also proportionally related to the thermal conductivity. Also, the lattice factor ( $\kappa_l$ ) represents the thermal conductivity resulting from the travel of vibrating phonons. When heat is applied, vibrating phonons travel with heat conduction through the lattice [7–10]. That is, when the obstruction of phonon transfer decreases the value of  $\kappa_l$ , a lower thermal conductivity is obtained. The literature contains numerous accounts of attempts to decrease thermal conductivity by inducing phonon scattering through methods such as atomic substitution, doping effects, and lattice manipulation, among other approaches [11–13].

In this respect, a porous structure is favorable to decrease thermal conductivity. As the electric factor, the pores have a role of obstacle to carrier transfer, resulting to decreased electrical conductivity with thermal conductivity. Also, in the lattice factor, it induces phonon scattering at the interface between the lattice and the pores. This scattering results in a decrease in thermal conductivity [14].

Various methods such as the breath-figure method, sol–gel process, and phase separation are often used to prepare porous structures [1, 15–21]. One of these methods, the organic/inorganic phase-separation-based sol–gel process, is particularly efficient because of its simple operation and low cost [22].

In this work, we used tetraethylorthosilicate (TEOS) and polyacrylonitrile (PAN) to fabricate porous structures for use in thermoelectric energy conversion devices via inorganic/organic nano-phase separation. We controlled the pore size

and morphology by varying the TEOS to PAN mixing ratio. Subsequent carbonization of the PAN matrix resulted in an electrically conductive structure.

## 2 Experimental Procedure

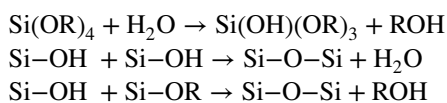
TEOS as precursor of silica particles and PAN ( $M_w$  150,000  $\text{g mol}^{-1}$ ) were purchased from Sigma-Aldrich Co.

TEOS dispersed into 0.02 M HCl and tetrahydrofuran (THF) (TEOS:HCl:THF = 1:5:12 (mole ratio)). The 3 wt% of PAN solution was prepared by dissolving in *N,N*-dimethylformamide (DMF) at 60 °C. The prepared TEOS solution was gradually added into the prepared PAN solution. In this step, the ratio of TEOS to PAN was controlled (TEOS: PAN = 3:1, 5:1, 6:1 and 7:1, w/w). The TEOS/PAN solution was subsequently dried under vacuum at 60 °C for 6 h. The electrically conductive structure was obtained by carbonization of the PAN matrix through heat treatment under an Ar environment at 850 °C for 3 h. The carbonized structure with silica particles was immersed in 5 wt% aqueous HF for 24 h to remove the silica particles for porous structure.

The fabricated porous structures were observed by field-emission scanning electron microscopy (FE-SEM, JSM-7401F, JEOL Ltd.). The porosity and pore size of each structure which fabricated with varying TEOS to PAN ratio was analyzed by using software of image J 1.50. Electrical conducting property was exploited by measuring electrical resistance of the structures by a digital multimeter (Fluke 175, Fluke Co.).

## 3 Results and Discussion

A schematic diagram of the process used to fabricate porous structures via TEOS/PAN phase separation was indicated at Fig. 1. Figure 2 shows the phase-separated structures of various weight ratio of TEOS to PAN from 3:1 to 7:1 (a, b, c and d). In the TEOS solution, Si–O–Si bridges are generated via hydrolysis and condensation reaction between TEOS and  $\text{H}_2\text{O}$ , resulting in formation silica nuclei and growth silica particles.



In this step, the acid environment controls the rate of hydrolysis and condensation, enabling the silica nuclei to grow into spherical particles [23, 24]. When a mixture of TEOS solution as silica nuclei and PAN solution is dried, silica particles grow via the Ostwald ripening effect. At that

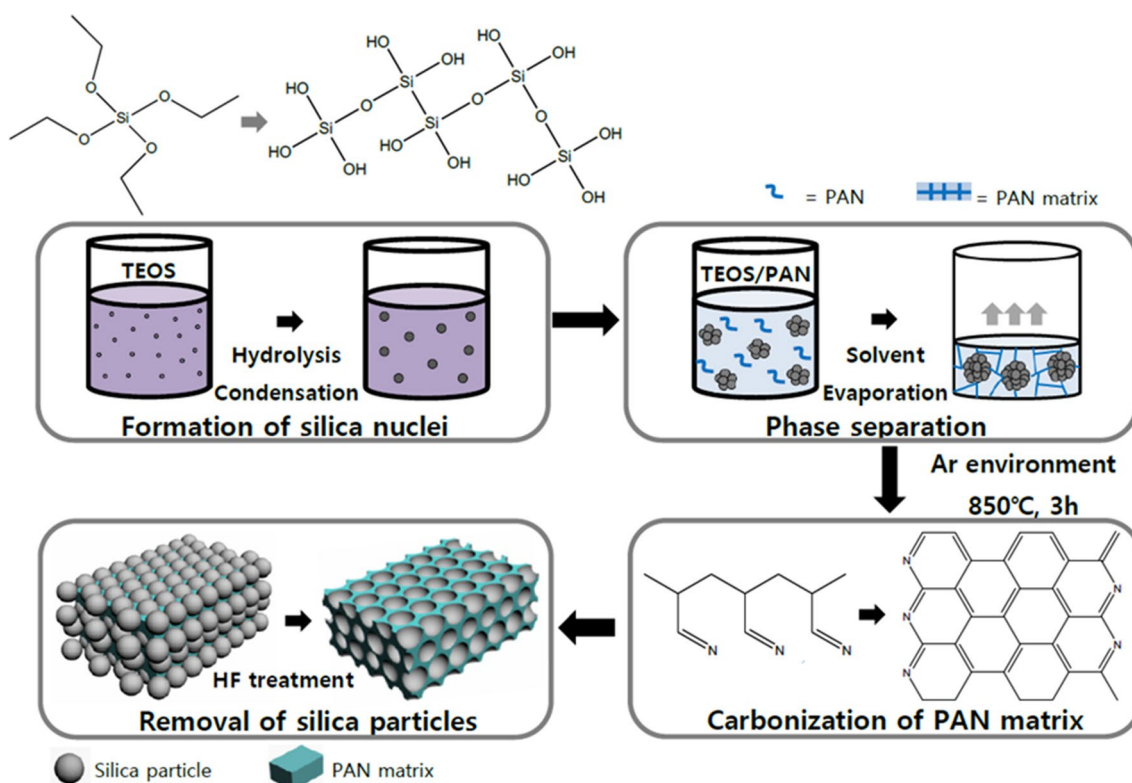


**Fig. 1** Schematic diagram of the fabrication of porous structures via TEOS/PAN phase separation

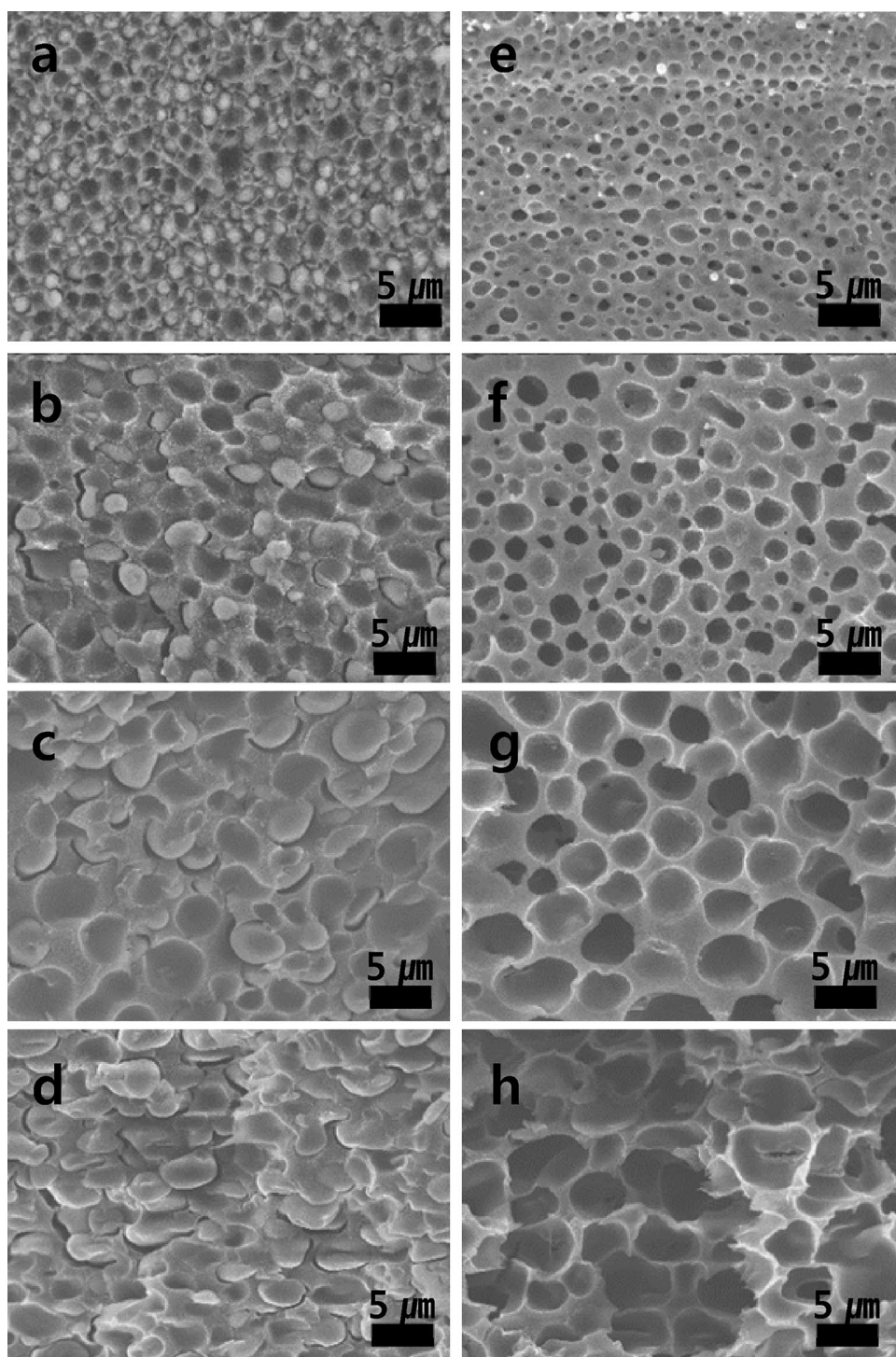
time, PAN is physically cross-linked with evaporation of the solvent by intermolecular dipole interactions between PAN chains due to polar nitrile groups [25], trapping the silica particles. Thus, the growth of the silica particles is limited by the cross-linked PAN structure and the particles are separated by the PAN matrix. After the phase separation and carbonization, porous structures were successfully fabricated by removal of silica particles with HF treatment (Fig. 1e–h).

The weight ratio of TEOS to PAN has an effect on size of formed silica particles in the phase separation step. Increased TEOS load to formation of larger particles compared to that of structure with low TEOS ratio (Fig. 1a–d). Because pores were formed by removal of the particles, the size of formed silica particles determined pore size with porosity in the structure. In the porous structure, increased size of pore from  $0.94 \pm 0.09$  to  $6.4 \pm 0.9$  ( $\mu\text{m}$ ) was obtained with increasing TEOS proportion to PAN from 3:1 to 7:1 (Fig. 3). With increase of pore size, porosity also increases at the higher TEOS ratios from 13.9 to 83.3 (%). The pore size and porosity were indicated in Table 1.

Electrically conductive porous structures were successfully fabricated with carbonization of PAN matrix. In Fig. 4, it was shown that electrical resistance of the porous structure with various TEOS ratio to PAN. The PAN matrix is commonly used for carbon structure because PAN exhibits high aromatic character and has a stabilized structure resulting

from polymerization of nitrile, which results in a high carbon yield after carbonization [26–28]. In the carbonization process of PAN, cyclization of  $-\text{C}\equiv\text{N}$ -bonds occurs at the proper temperature and results in  $-\text{C}=\text{N}$ -bonds. A continuous ladder structure is formed by dehydrogenation. Under an inert-gas atmosphere at high temperatures, cyclic carbon compounds are obtained through the formation of  $-\text{C}=\text{C}$ -bonds and denitrogenation of the ladder structure [29, 30]. As the results, resistance was increased from  $90 \pm 8$  ( $\Omega$ ) at ratio of TEOS to PAN is 3:1 to maximum  $300 \pm 40$  ( $\Omega$ ) at 5:1 with increased porosity. Usually, it has been reported that carbonized PAN films had about 180–840 (S/cm) of electrical conductivity [26]. It means that carriers transport in our porous carbonized films was hindered by micro sized-pores, however, it showed still reasonable electrical conductivities. It will be expected to have to show a decrease in an electric factor of their thermal conductivities (Fig. 5) [31, 32]. In the following studies, it is expected that this porous structure also hinders effectively phonon transport with decrease of lattice factor in thermal conductivity, which leads to highly effective thermoelectric devices [33].

**Fig. 2** The morphologies of phase separated structure (**a**, **b**, **c** and **d**) between silica particles and PAN matrix and porous structures (**e**, **f**, **g** and **h**) after removal of silica particles in carbonized PAN matrix with various the weight ratio TEOS to PAN of 3:1 (**a**, **e**), 5:1 (**b**, **f**), 6:1 (**c**, **g**) and 7:1 (**d**, **h**)



## 4 Conclusions

Porous structures which favorable to decrease thermal conductivity as thermoelectric energy conversion materials were fabricated via inorganic/organic nano-phase separation. The formation of silica particles was controlled by varying the mixing ratio of TEOS as a precursor to silica particles to PAN. Higher TEOS to PAN weight ratios resulted in porous

structures with larger pore sizes because the content of PAN, which limits the growth of silica particles, relatively decreases. As the results, porous structures having from 13.9 to 83.3 (%) of porosity were successfully obtained. Additionally, the structures had electrical conductive properties by carbonizing the PAN matrix. With increased porosity, electrical resistance was increased  $90 \pm 8$  to  $300 \pm 40$  ( $\Omega$ ) which lead to decrease electric factor of thermal conductivity. It



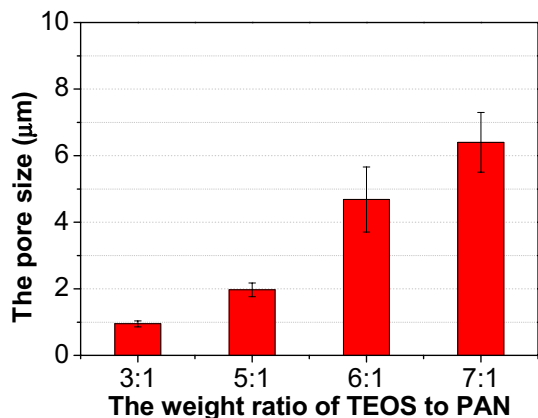


**Fig. 3** The difference of pore size in the fabricated porous structures by TEOS weight ratios to PAN

**Table 1** The pore size and porosity with various TEOS weight ratio to PAN

TEOS: PAN (w/w)	Pore size (µm)	Porosity (%)
3:1	0.94 ± 0.09	13.9
5:1	2.0 ± 0.2	20.3
6:1	4.7 ± 0.9	52.0
7:1	6.4 ± 0.9	83.3

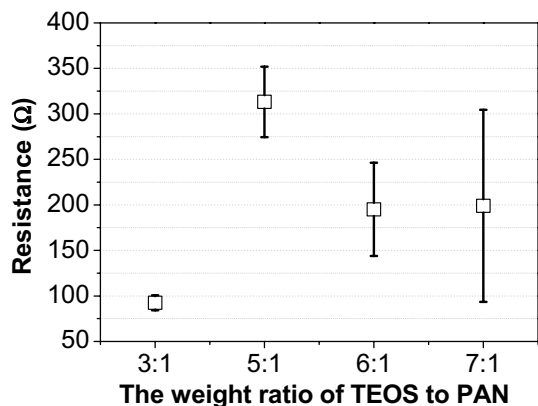


**Fig. 4** The resistance of the conductive porous structures with variation of TEOS ratios to PAN

means that formed micro-sized pores had a role of obstacles to carrier transfer in the conductive matrix. In addition, it is expected that this structures are also efficient to induce phonon scattering with decrease lattice factor of thermal conductivity. However, because decreased electrical conductivity is also related to lower ZT, independent control of lattice factor is required. The fabricated conductive porous structure is expected to be applied in various field as well as thermoelectric device due to its structural advantages such

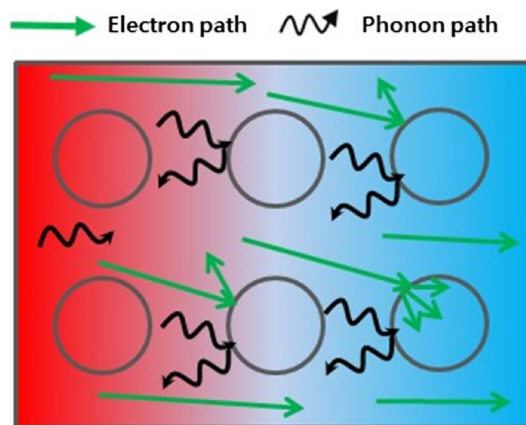


**Fig. 5** Schematic diagram of electron and phonon path in macroporous structure

as high surface area with porosity, electrical conductive property by carbonization and so on.

**Acknowledgements** This research was supported by Basic Science Research Program through the National Research Foundation of Korea (NRF) funded by the Ministry of Science and ICT (NRF-2017R1A2B2010552 and 2015R1A5A7037615) and Civil Military Technology Cooperation Center (15-CM-SS-03 and 15-CM-EN-08).

**References**

- Naboka, O., Sanz-Velasco, A., Lundgren, P., Enoksson, P., Gatenholm, P.: Cobalt (II) chloride promoted formation of honeycomb patterned cellulose acetate films. *J. Colloid Interface Sci.* **367**, 485 (2012)
- Li, Y., Fu, Z.Y., Su, B.L.: Hierarchically structured porous materials for energy conversion and storage. *Adv. Funct. Mater.* **22**, 4634 (2012)
- Zukalova, M., Zukal, A., Kavan, L., Nazeeruddin, M.K., Liska, P., Grätzel, M.: Organized mesoporous TiO<sub>2</sub> films exhibiting greatly enhanced performance in dye-sensitized solar cells. *Nano Lett.* **5**, 1789 (2005)
- Liu, W., Chen, Z., Zhou, G., Sun, Y., Lee, H.R., Liu, C., Yao, H., Bao, Z., Cui, Y.: 3D porous sponge-inspired electrode for stretchable lithium-ion batteries. *Adv. Mater.* **28**, 3578 (2016)
- Wolf, A., Brendel, R.: Thermal conductivity of sintered porous silicon films. *Thin Solid Films* **513**, 385 (2006)
- Snyder, G.J., Toberer, E.S.: Complex thermoelectric materials. *Nat. Mater.* **7**, 105 (2008)
- Cornett, J.E., Rabin, O.: Thermoelectric figure of merit calculations for semiconducting nanowires. *Appl. Phys. Lett.* **98**, 182104 (2011)
- Cornett, J.E., Rabin, O.: Universal scaling relations for the thermoelectric power factor of semiconducting nanostructures. *Phys. Rev. B* **84**, 205410 (2011)
- Li, J.F., Liu, W.S., Zhao, L.D., Zhou, M.: High-performance nanostructured thermoelectric materials. *NPG Asia Mater.* **2**, 152 (2010)
- Shu, J., Xia, R., Qian, J., Miao, J., Su, L., Cao, M., Lin, H., Chen, P., Chen, J.: Preparation and study on thermal conductive

- composites of chlorinated polyethylene rubber reinforced by boron nitride particles. *Macromol. Res.* **24**, 640 (2016)
11. Kim, W., Zide, J., Gossard, A., Klenov, D., Stemmer, S., Shakouri, A., Majumdar, A.: Thermal conductivity reduction and thermoelectric figure of merit increase by embedding nanoparticles in crystalline semiconductors. *Phys. Rev. Lett.* **96**, 045901 (2006)
  12. Tang, J., Wang, H.-T., Lee, D.H., Fardy, M., Huo, Z., Russell, T.P., Yang, P.: Holey silicon as an efficient thermoelectric material. *Nano Lett.* **10**, 4279 (2010)
  13. Kim, H., Lee, J.K., Park, S.D., Ryu, B., Lee, J.E., Kim, B.S., Min, B.K., Joo, S.J., Lee, H.W., Cho, Y.-R.: Enhanced thermoelectric properties and development of nanotwins in Na-doped Bi<sub>0.5</sub>Sb<sub>1.5</sub>Te<sub>3</sub> alloy. *Electron. Mater. Lett.* **12**, 290 (2016)
  14. Lee, J.H., Galli, G.A., Grossman, J.C.: Nanoporous Si as an efficient thermoelectric material. *Nano Lett.* **8**, 3750 (2008)
  15. Lee, S.H., Park, J.S., Lim, B.K., Mo, C.B., Lee, W.J., Lee, J.M., Hong, S.H., Kim, S.O.: Highly entangled carbon nanotube scaffolds by self-organized aqueous droplets. *Soft Matter* **5**, 2343 (2009)
  16. Warren, S.C., Perkins, M.R., Adams, A.M., Kamperman, M., Burns, A.A., Arora, H., Herz, E., Suteewong, T., Sai, H., Li, Z.: A silica sol–gel design strategy for nanostructured metallic materials. *Nat. Mater.* **11**, 460 (2012)
  17. Johnson, S.A., Ollivier, P.J., Mallouk, T.E.: Ordered mesoporous polymers of tunable pore size from colloidal silica templates. *Science* **283**, 963 (1999)
  18. Imhof, A., Pine, D.: Ordered macroporous materials by emulsion templating. *Nature* **389**, 948 (1997)
  19. Cui, L., Peng, J., Ding, Y., Li, X., Han, Y.: Ordered porous polymer films via phase separation in humidity environment. *Polymer* **46**, 5334 (2005)
  20. Jung, D., Cho, S.G., Moon, T., Sohn, H.: Fabrication and characterization of porous silicon nanowires. *Electron. Mater. Lett.* **12**, 17 (2016)
  21. Kim, S., Kwag, D.S., Lee, D.J., Lee, E.S.: Acidic pH-stimulated tiotropium release from porous poly(lactic-co-glycolic acid) microparticles containing 3-diethylaminopropyl-conjugated hyaluronate. *Macromol. Res.* **24**, 176 (2016)
  22. Lee, J.P., Choi, S., Park, S.: Preparation of silica nanospheres and porous polymer membranes with controlled morphologies via nanophase separation. *Nanoscale Res. Lett.* **7**, 1 (2012)
  23. Brinker, C.J., Keefer, K.D., Schaefer, D.W., Ashley, C.S.: Sol-gel transition in simple silicates. *J. Non Cryst. Solids* **48**, 47 (1982)
  24. Nakanishi, K.: Pore structure control of silica gels based on phase separation. *J. Porous Mat.* **4**, 67 (1997)
  25. Tan, L., Pan, D., Pan, N.: Gelation behavior of polyacrylonitrile solution in relation to aging process and gel concentration. *Polymer* **49**, 5676 (2008)
  26. Zhou, Z., Lai, C., Zhang, L., Qian, Y., Hou, H.: Development of carbon nanofibers from aligned electrospun polyacrylonitrile nanofiber bundles and characterization of their microstructural, electrical, and mechanical properties. *Polymer* **50**, 2999 (2009)
  27. Fitzer, E., Frohs, W., Heine, M.: Optimization of stabilization and carbonization treatment of PAN fibres and structural characterization of the resulting carbon fibres. *Carbon* **24**, 387 (1986)
  28. Rahaman, M.S.A., Ismail, A.F., Mustafa, A.: A review of heat treatment on polyacrylonitrile fiber. *Polym. Degrad. Stab.* **92**, 1421 (2007)
  29. Nataraj, S., Yang, K., Aminabhavi, T.: Polyacrylonitrile-based nanofibers—a state-of-the-art review. *Prog. Polym. Sci.* **37**, 487 (2012)
  30. Chen, J., Harrison, I.: Modification of polyacrylonitrile (PAN) carbon fiber precursor via post-spinning plasticization and stretching in dimethyl formamide (DMF). *Carbon* **40**, 25 (2002)
  31. Cuevas, F.G., Montes, J.M., Cintas, J., Urban, P.: Electrical conductivity and porosity relationship in metal foams. *J. Porous Mater.* **16**, 675 (2008)
  32. Chung, W.H., Hwang, H.J., Kim, H.S.: Flash light sintered copper precursor/nanoparticle pattern with high electrical conductivity and low porosity for printed electronics. *Thin Solid Films* **580**, 61 (2015)
  33. Bark, H., Lee, J., Lim, H., Koo, H.Y., Lee, W., Lee, H.: Simultaneous nitrogen doping and pore generation in thermo-insulating graphene films via colloidal templating. *ACS Appl. Mater. Interfaces* **8**, 31617 (2016)